Analyzing powers for $\pi^{\pm}$-$^{13}\vec{C}$ scattering at $T_\pi = 100$ MeV

J. T. Brack, A. Feltham, R. R. Johnson, G. Jones, M. A. Kermani, O. Meirav,*
M. Pavan, M. E. Sevior, V. Sossi, D. Vetterli,† and P. Weber‡
University of British Columbia, Vancouver, British Columbia, Canada V6T 1Z1

G. R. Smith, P. A. Amaudruz, D. Healey, D. F. Ottewell, and Y. S. Wu§
TRIUMF, Vancouver, British Columbia, Canada V6T 2A3

X. Y. Chen, S. Høibråten, M. D. Kohler, J. J. Kraushaar, R. A. Ristinen, and W. R. Smythe
University of Colorado, Boulder, Colorado 80309

E. L. Mathie and D. M. Yeomans
University of Regina, Regina, Saskatchewan, Canada S4S 0A2

R. Schubank and N. R. Stevenson**
University of Saskatchewan, Saskatoon, Saskatchewan, Canada S7N 0W0

E. F. Gibson
California State University, Sacramento, California 95819
(Received 21 August 1991)

Measurements of the analyzing power for the $^{13}\vec{C}(\pi^{\pm},\pi^{\pm})$ reaction at $T_\pi = 100$ MeV have been made at TRIUMF using a polarized target consisting of 99% ^{13}C enriched butanol. Data were obtained for the ground and 3.68 MeV excited states at angles from 110° to 150° in 10° steps. The data are consistent with zero asymmetry throughout most of this angular range. Uncertainties are typically ±15%, which is sufficient to discriminate among some, but not all, of the currently available theoretical predictions.

PACS number(s): 25.40.Dn, 24.70.+s

I. INTRODUCTION

Although polarized beams of leptons and hadrons have been available for many years it is only recently that polarized nuclear targets of $A > 2$ nuclei have become available, thus making possible the measurement of spin observables using the spin-zero pion as a probe. The first few experiments involving pion scattering from polarized nuclear targets at Paul Scherrer Institute (PSI) and LAMPF have recently been published [1–5]. We report here on the first in a planned series of TRIUMF experiments using polarized nuclear targets, measuring pion scattering analyzing powers for the $\frac{1}{2}^-$ ground and $\frac{3}{2}^-$ 3.68 MeV excited states of polarized ^{13}C, at angles near the second minimum in the ^{13}C elastic cross section.

Since the meson facilities came on line in the mid 1970s a large body of pion-nucleus differential cross section data has been accumulated. The differential cross sections are proportional to the sum of the squares of two scattering amplitudes, f and g, describing the non-spin-flip and spin-flip contributions to the interaction. The non-spin-flip amplitude (f) dominates the cross-section observable at most scattering angles, while the relatively small spin-flip amplitude (g) gains prominence near the diffractive minima of the cross-section angular distribution, where the contribution from f is small. Unfortunately, this is precisely where measurements of this observable are most difficult, leaving the amplitude g experimentally ill-defined.

Under these conditions, a variety of models using different spin-flip amplitudes can be optimized to generate reasonable agreement with the cross-section data. But these models may then have large discrepancies in the predictions of spin observables. The polarization asymmetry observable A_y is defined as

$$A_y(\theta) = \frac{\sigma^{\uparrow}(\theta) - \sigma^{\downarrow}(\theta)}{P^{\downarrow}\sigma^{\uparrow}(\theta) + P^{\uparrow}\sigma^{\downarrow}(\theta)} = \frac{2\,\mathrm{Im}(fg^*)}{|f(\theta)|^2 + |g(\theta)|^2}\ , \qquad (1)$$

where $\sigma^{\uparrow}(\theta)$ denotes the measured differential cross section from a target with polarization $P^{\uparrow}$. In contrast to the expression for the cross section, it is the product and relative phase of the f and g amplitudes that determine A_y. Further, A_y is seen to be inversely proportional to the spin-averaged cross section, thus enhancing the dependence on g near the diffractive cross-section minima where f is small. It is expected that measurements of

*Present address: Elscint, Haifa, Israel.
†Present address: Institute for Physics, University of Basel, CH-4056 Basel, Switzerland.
‡Present address: IMP/ETH Zürich, PPE-Div CERN, 1211 Geneva 23, Switzerland.
§Present address: Institute of Atomic Energy, P.O. Box 275 (43), Beijing, P.R. China.
**Present address: TRIUMF, Vancouver, British Columbia, Canada V6T 2A3.

spin observables will assist the refinement of the various models.

Several calculations of A_y existed in advance of the first experimental data. The models used to make these predictions fall into three groups [6]: those working in coordinate space with zero-range interactions [7], those working in momentum space using optical model or similar nonlocal potentials [8–10], and delta-hole models which explicitly treat the formation and propagation of the Δ particle through the nucleus under the influence of a Δ-nucleus potential [6,11,12].

While in general the ability of these models to predict measured spin observables is poor, there has been some success. The ^{6}Li asymmetry calculations by Mach predict the general features of the recent data [3]. However, the same model predicts large ^{15}N asymmetries at angles near the cross-section minima, while the measured asymmetries are consistent with zero [2]. The distorted-wave impulse approximation (DWIA) calculations of Chakravarti [9] provide a reasonable description of the small angle ^{13}C data at $T_\pi = 132$ MeV [4] but not of data at larger momentum transfer at $T_\pi = 132$ or 100 MeV, as discussed below. The asymmetries predicted at 100 MeV by these models differ as much as 0.7 near 115° pion scattering angle.

II. THE EXPERIMENT

The experiment was performed on the M11 channel at TRIUMF [13], tuned to deliver 100 MeV pions at the center of the experimental target. A 2.1 mm thick CH_2 degrader was placed near the channel midplane to eliminate protons from the beam. For positive channel polarity, the horizontal slits at the channel midplane were adjusted so that the momentum acceptance $\Delta p/p$ was 1.0%, giving a spread ΔT in incident pion energies of 1.6 MeV. For negative polarity, the slits were opened to increase the beam rate, giving a $\Delta p/p$ of 1.5%, or ΔT of 2.4 MeV. Typical rates were between 0.5×10^6 and 1.0×10^6 π/s.

Beam incident on the target was defined by a single scintillator S (see Fig. 1). A discriminator setting $\bar{S}$ eliminated events with S pulse heights a factor of 4 or more above the single pion pulse height, thus removing from the analysis any events triggered by protons that may have passed through the channel in spite of the midplane degrader. A coincidence $S\cdot\bar{S}$ defined the beam scaler. Beam parameters were sampled at regular intervals by a separate clock controlled circuit. At each coincidence of beam with this clock, all beam related parameters were written to tape.

Scattered particles were detected in the quadrupole-quadrupole-dipole (QQD) spectrometer [13], used near the upper end of its 200 MeV/c momentum range. The angular range of the QQD, normally limited to laboratory angles less than 135° by physical obstacles, was enlarged by the rotation of particle trajectories in the target magnetic field, permitting measurements at angles as large as 150° (see Fig. 1). The large radius of the target cryostat outer vacuum window dictated that the first wire chamber and quadrupole magnet be removed from the

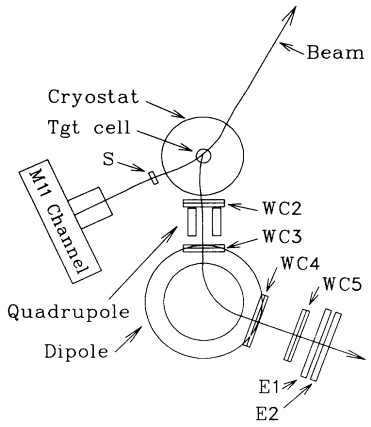

FIG. 1. The experimental layout, showing the orientation of the spectrometer for a scattering angle of 150°, and the pion trajectories in the spectrometer and in the 2.55 T target field.

spectrometer front end to accommodate the polarized target. This first (vertically focusing) quadrupole was moved back to the position normally occupied by the second (horizontally focusing) quadrupole. Particle trajectories through the spectrometer were recorded by means of the four wire chambers. All wire chambers used delay line readout to obtain position information. Information on the vertical position of the tracks was obtained from horizontal anode wires, thus limiting the vertical resolution to the 2 mm anode wire spacing. Horizontal position information came from vertical cathode wires. The cathode spacing was 1 mm for WC2 and WC3, and 2 mm for WC4 and WC5. The resulting induced pulses on a cluster of these vertical cathode wires provided horizontal position resolution much better than the spacing. Two scintillators ($E1$ and $E2$) were placed behind the last wire chamber (WC5). A coincidence $E1\cdot E2$ defined a spectrometer event, and this in coincidence with a beam event provided the event trigger for the experiment.

The target was a modified version of a butanol (C_4H_9OH) target used previously at TRIUMF for pion scattering experiments from polarized protons [14] and deuterons [15] and has been described in detail in those works. For the deuteron experiment the ^{1}H content of the butanol was replaced with deuterium. For the present work a butanol compound was used in which the carbon content was 99% ^{13}C enriched. The magnetic moments of these nuclei are $2.793\mu_N$ (proton), $0.8574\mu_N$ (deuteron), and $0.702\mu_N$ (^{13}C). A brief description of the target and its modifications follows.

The target cell consisted of a $22\times15\times5$ mm^3 rectangular box constructed of 50 μm thick mylar. This cell could slide in and out of a second slightly larger cell of 25 μm thick mylar, which supported a coil of 50 μm diameter copper wire, employed in the NMR circuit. This assembly was supported by a third mylar layer, which also supported a second identical (dummy) assembly, mounted several centimeters below the first. The butanol beads, formed by allowing drops of liquid butanol to fall into liquid nitrogen, were placed in the upper cell. When installed for the experiment, the entire assembly could be

raised, allowing the lower cell to be used as a background target. The stationary superconducting polarizing coils were mounted in the target cryostat above and below the target cell. The cell was immersed in the cylindrical bath of a ^{3}He-^{4}He dilution refrigerator, contained by a 0.15 mm thick aluminum wall of 13.25 mm radius. The bath was surrounded by a vacuum chamber containing several layers of copper heat shielding. The outer vacuum window was at a radius of about 30 cm. The temperature in the target cell was typically 100 mK.

Polarization was achieved in a 2.55 T magnetic field by irradiation with microwaves at frequencies of 70.450 GHz (positive polarization state, with spin parallel to **B**) or 70.870 GHz (negative state). It should be pointed out that the direction of the target magnetic field is the same for either polarization, and thus the pion trajectories were unaffected by polarization changes. The reduced field, or "frozen spin" mode, was not used, and pion scattering data were taken with the target field at 2.55 T. The target polarization was calibrated using the thermal equilibrium technique, which involves comparing the area of the ^{13}C NMR signal when dynamically polarized to the area of the signal at thermal equilibrium. The area is related to the polarization, which can be determined independently at thermal equilibrium from a knowledge of the temperature and magnetic field [14]. The area of the NMR signal was monitored throughout each run, and was recorded on tape at regular intervals to facilitate the polarization calculations. Typical polarizations achieved during the experiment were $27\pm2\%$ for the positive state and $29\pm2\%$ for the negative state.

Three explicit background measurements were made at each spectrometer setting and pion polarity to account for the three primary sources of background in this experiment: helium, oxygen, and the target cell. The first of these, liquid ^{4}He, was performed on completion of the foreground measurements for each pion polarity. The target ladder was raised a few centimeters within the cryostat to position the (empty) dummy target cell in the pion beam, and data were gathered under conditions otherwise identical to those for the foreground measurements. The remaining two backgrounds were measured after all foreground and ^{4}He data runs were completed, at which time the liquid helium was pumped from the cryostat. The target ladder was removed from the cryostat and the upper cell was filled with spheres of ice, formed by allowing drops of water to freeze in liquid nitrogen. The lower target cell remained empty. The target ladder was then inserted back into the cryostat, and the backgrounds associated with each target were measured.

A few comments should be made about the limitations of the above described apparatus. First, the relatively long time ($\sim$ six hours) necessary for target polarization precluded the use of our preferred data taking sequence. In most previous experiments by this group, the target was polarized in a sequence of orientations symbolized by $+--++--+$ before moving to the next angle. The multiple runs for each target polarity allow checks on systematic uncertainties. Here, time constraints dictated that data be acquired at several angles before flipping the polarization of the target, with the result that the polarization sequence for the various runs at a given angle was modified to $++--$, and these runs were spread over a period of weeks. Second, at this momentum setting it is not possible to get both the πp elastic and the ^{13}C elastic peaks on the focal plane of the QQD spectrometer at the same time. This eliminated the possibility of using the known πp polarization asymmetries [14] as a systematic check.

Several factors contributed to the overall energy resolution. The greatest single contribution was due to the large $\Delta p/p$ setting for the channel necessary to obtain reasonable fluxes, as mentioned above, producing energy spreads of 1.6 and 2.4 MeV (FWHM) in the incident pion energies for the π^+ and π^- data, respectively. For the large-angle measurements reported here, it was necessary to use a reflection geometry for the target, in which the degradation of the resolution is much larger than for a transmission geometry. The contribution is twice the energy loss in the scattering material, and here amounted to between 1.2 and 1.6 MeV depending on the scattering angle. Finally, the removal of the first wire chamber worsened the nominal 1.1 MeV resolution of the QQD spectrometer to an estimated 1.5 MeV. The above factors resulted in an intrinsic resolution of between 2.5 and 3.2 MeV, depending on angle and pion polarity, and dominate the widths observed in the final spectra.

III. DATA ANALYSIS

Several software restrictions (cuts) were applied to the raw scattering data. The cyclotron rf referenced time of flight (TOF) through the M11 channel was used to measure the pion fraction of the incident beam. In addition, the TOF information was used to eliminate from the analysis the few scattering events caused by particles other than pions. Using information from the two QQD front-end wire chambers, it was possible to construct histograms of the scattering vertex in the target cell, and to define a cut centered on the butanol content of the target. The resolution of these spectra was not optimum due to the modified front end of the spectrometer, and when the cut was adjusted to eliminate most of the scattering from the helium and target cell, it then also eliminated a substantial fraction of the foreground scattering. Although this cut was not used in the final analysis in order to obtain better statistics, application of this cut would not have changed the final results by more than one standard deviation for any given point.

To reduce the number of events in which scattered pions decayed in the spectrometer, a cut was applied to spectra of the difference in position at the last two spectrometer wire chambers, where a peak representing the range of slopes corresponding to pion trajectories was observed. A similar cut was applied in both the x and y chamber dimensions. This could be done only in the case where both of these chambers fired. For the remaining $\sim$20% of events, no such cut was applied.

A missing mass spectrum was formed from the events remaining after the above cuts. Corrections were included for the kinematic spread in scattered pion energy over the $\pm5^\circ$ acceptance of the spectrometer.

All data were analyzed as described above. Small energy shifts were made to the background and empty-target histograms to compensate for pion energy loss variations in the target. The beam-normalized empty-target spectra were then subtracted from those of the foreground and oxygen runs. Finally, the oxygen background was normalized for beam and target thickness and subtracted from the foreground spectra. The resulting spectra should contain only scattering events from helium and ^{13}C, but in practice a small amount of heavy-nucleus scattering remained to the right of the ^{13}C ground-state peak. The location of these remaining events in the missing mass histogram is consistent with scattering from copper, and could result from slightly different NMR windings in the foreground and dummy target cells. As seen in Figs. 2 and 3, the helium peak was split into two distinct scattering energies due to the reflection-mode target geometry. The left-hand peak corresponds to pions which traveled through the butanol in the target and backscattered in the helium downstream, thus traveling twice through the butanol before entering the spectrometer. The peak to the right of this corresponds to pions which scattered from the helium upstream of the butanol. This splitting of the helium peak in the foreground spectra made it virtually impossible to make use of the measured helium background spectra. In the kinematic region explored here, only the ground and 3.68 MeV excited states of ^{13}C contribute significantly to the spectrum. Thus five Gaussians were used to fit the spectra: two for helium, one each for the ^{13}C ground and 3.68 MeV excited states, and one for the residual scattering from heavy nuclei in the target, as shown in Fig. 3. The fitting procedure assumed there was no background in this region.

In principle, the fitting procedure described above should have included peaks corresponding to the 3.09 MeV ($\frac{1}{2}^+$) and 3.85 MeV ($\frac{5}{2}^+$) states surrounding the 3.68 MeV state. These states are not resolved in the present experiment, and thus the asymmetries reported here for the 3.68 MeV state are combined results for the three states. However, previous experiments at incident pion energies of 100 MeV [16] and 65 MeV [17] with unpolarized targets and resolution of 800 and 500 keV, respectively, suggest that the spin-averaged cross sections for these positive-parity states are negligible relative to the 3.68 MeV state. (For incident pions at resonance energy this may not be the case [18].) If it is estimated that these peaks contribute as much as 5% to the area of the 3.68 MeV peak when a single Gaussian is used for the fit, then the maximum effect on the 3.68 MeV state asymmetries observed here would be 0.05 for the extreme case of $A_y = 1.0$ for this additional 5% area. This is small compared to the present experimental uncertainties for this state.

As a systematic check on the subtraction process outlined above, the normalized raw spin-down spectra were subtracted from the spin-up spectra, as shown in the lower portion of Fig. 3 for a typical case. Integration of the resulting difference spectrum over the ground state or 3.68 MeV excited state region provided a quantity proportional to the numerator of the asymmetry expression, which could be compared to the equivalent quantity calculated from the fitting technique. This difference method minimizes uncertainties associated with the background subtractions, or with the peak fitting routine. In all cases, the results from the two methods agreed within the uncertainties calculated for the five Gaussian fit method. The uncertainty in the area of each ^{13}C peak was derived from a quadrature addition of the statistical uncertainties of the fitting routine with twice the background area contributed by surrounding Gaussians.

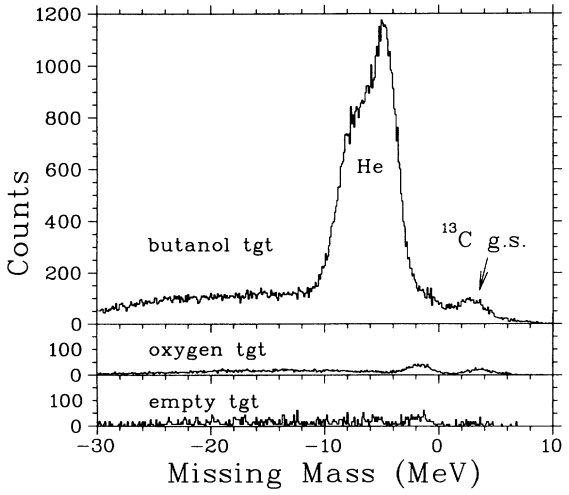

FIG. 2. A sample spectrum of the reconstructed missing mass for the foreground butanol target showing the associated background target contributions, as measured in separate runs. The background runs have been normalized as described in the text. The pion scattering angle was 130°_{lab}. A cut eliminating scattering from the target pillars has been applied to these data.

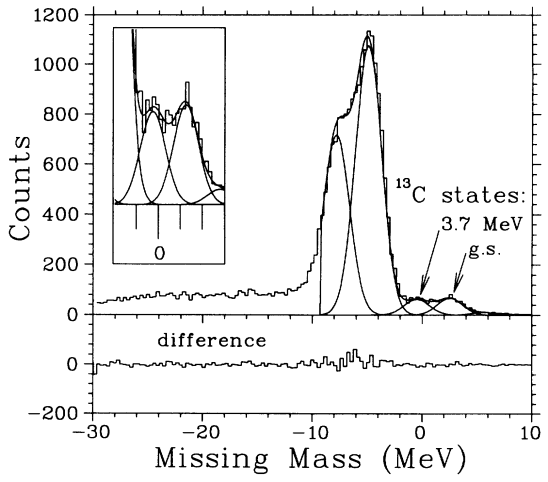

FIG. 3. A sample spectrum of the final data, showing the fit from which the yields were extracted. This spectrum is the final result after subtraction of the data shown in the previous figure. No additional cut has been applied. Below this is a sample of the difference spectra, formed from the normalized difference of the raw spin-up and spin-down missing mass histograms. No cuts or background subtractions were applied before the difference was taken.

IV. RESULTS AND DISCUSSION

The average of the spin-up and spin-down relative cross sections for the ^{13}C ground state and 3.68 MeV excited state obtained from the fits described above are displayed in Figs. 4(a) and 5(a), along with the spin-averaged absolute differential cross sections measured by Antonuk *et al.* [16]. The present data were normalized to the cross sections of Antonuk *et al.* for the 3.68 MeV excited state, where the angular distribution is flat. In general, the present measurements for the 3.68 MeV state track with the absolute cross sections of Ref. [16], but the ground-state cross sections appear low at back angles compared to the absolute cross sections. We have no explanation for this discrepancy.

Also shown in Figs. 4(a) and 5(a) are predicted cross sections from the models of Siegel, Chakravarti, and Mach and Kamalov. The predictions of Siegel [7] (long-short-dashed line) were generated from a coordinate-space model using the distorted-wave Born approximation [19]. The calculations used a first-order optical potential and distorted waves from an optical model [20] including medium modifications. The predictions of Chakravarti [9] (short-dashed line) are momentum-space calculations using the distorted-wave impulse approximation (DWIA). No medium corrections were included. The elastic π-nucleus amplitude was obtained using shell-model transition densities from Cohen and Kurath [21]. A first-order optical potential generated the distorted waves using ground-state densities from electron scattering. A third model, that of Mach and Kamalov [10], is a DWIA calculation similar to that of Ref. [9], but a phenomenological second-order term was added to the optical potential to account for absorption and higher-order effects. Two predictions were generated from this model, corresponding to the use of different wave functions as input (solid line is from Cohen-Kurath [21] wave functions and long-dashed line is from those of Tiator [22]). Although the agreement between the calculations of each of these models and the measured cross sections might be characterized as poor at forward scattering angles, the descriptions are entirely inadequate [16] at the comparatively large angles presented here and miss at extreme back angles by between one and two orders of magnitude.

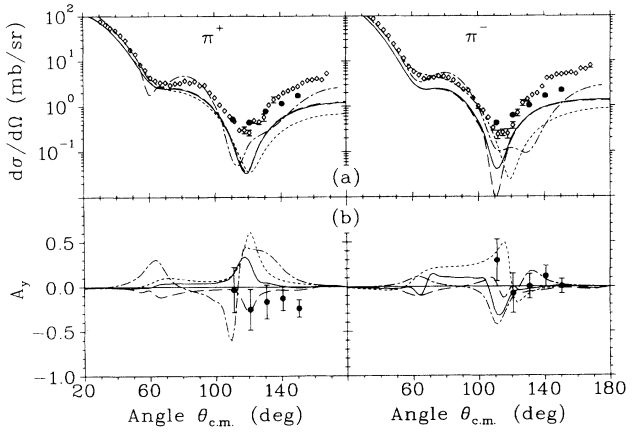

FIG. 4. The ground-state spin-averaged relative cross sections (a) and the polarization asymmetries A_y (b) are shown for $^{13}\vec{C}(\pi^{\pm},\pi^{\pm})$ scattering at $T_\pi = 100$ MeV, as measured in this experiment (solid symbols). In (a), the absolute cross sections of Antonuk *et al.* [16] (open diamonds) are shown for comparison. The curves are from the predictions of the models of Mach [10] (solid line is for Cohen-Kurath wave functions [19], long-dashed line is for Tiator wave functions [20]), Chakravarti [9] (short-dashed line is for Cohen-Kurath wave functions [19]) and Siegel [7] (long-short-dashed line). Error bars on the present data reflect statistical uncertainties, added in quadrature with those from background subtraction.

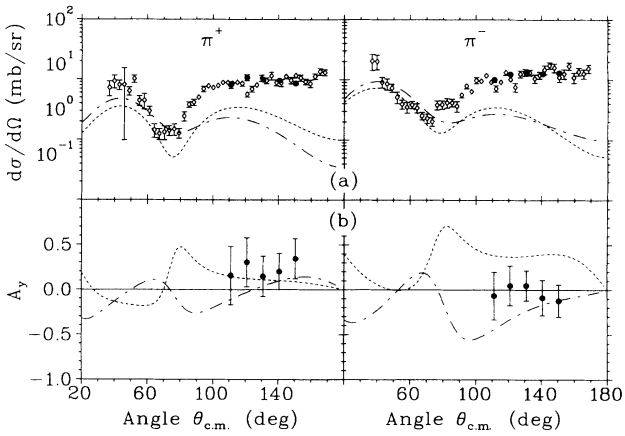

FIG. 5. As in Fig. 4, but for the 3.68 MeV excited state.

It is perhaps no surprise then that there is also no consistently accurate description of the asymmetries, shown in Figs. 4(b) and 5(b) and listed in Table I. The model of Chakravarti [9], which does well for small momentum transfer data at $T_\pi = 132$ MeV [4], predicts large positive values for A_y at 100 MeV of between 0.5 and 0.6 for both π^+ and π^- at angles near the second minimum of the elastic cross section. While the predictions of this model are in good agreement with the present ground-state π^- asymmetry data, the π^+ data imply negative values for A_y, and lie three standard deviations below the prediction. In both cases, the data are within 1.5 standard deviations of consistency with zero asymmetry. The present A_y data for π^- are consistent with those of Yen *et al.* [4]

TABLE I. The polarization asymmetries A_y for $^{13}C(\pi^{\pm},\pi^{\pm})^{13}C$ scattering for the ground and 3.68 MeV excited states at $T_\pi = 100$ MeV.

θ_π c.m. (deg)	Polarity	A_y (g.s.)	A_y (3.68 MeV)
110	π^+	−0.03±0.25	0.16±0.32
120	π^+	−0.25±0.23	0.30±0.27
130	π^+	−0.17±0.19	0.15±0.23
140	π^+	−0.13±0.11	0.20±0.20
150	π^+	−0.24±0.10	0.34±0.22
110	π^-	0.29±0.23	−0.08±0.24
120	π^-	−0.07±0.22	0.04±0.22
130	π^-	0.00±0.14	0.05±0.17
140	π^-	0.12±0.11	−0.10±0.20
150	π^-	−0.00±0.08	−0.14±0.18

at slightly higher energy ($T_\pi = 114$ MeV), although the 14 MeV difference in incident pion energy is perhaps too large for a reliable comparison. For example, the predictions of Ref. [9] between 100° and 120° vary severely between 100 and 132 MeV. Although spin matrix quenching factors were used in that model in an attempt to fit ^{15}N data [9], none were used for the present calculation, and none were necessary for a resonable fit to the ^{13}C data at $T_\pi = 132$ MeV [4]. Quenching of spin matrix elements on the order of 30–40 % has been found necessary in models describing (e,e'), (p,p'), and (p,n) reactions [23]. For the 3.68 MeV excited state, the agreement of this model with the π^+ data is good, but the π^- asymmetries are consistent with zero at all five angles while the predictions are constant in this region at ~ 0.5.

The results of a preliminary calculation by Siegel [7] deviate from the measured ground-state A_y data for both pion polarities. For π^- the agreement is good with the elastic data at the larger four scattering angles, but not at 110°, where the cross section is very near the minimum. Here, the predicted A_y is near -0.4, while the data imply a positive value. The π^+ elastic predictions, like those of Ref. [9], are large and positive where the data are negative. In addition, the corresponding cross-section predictions oscillate near the second minimum.

The Mach and Kamalov prediction using the wave functions of Tiator provides a better description of the ground-state data, but no 3.68 MeV excited-state predictions are currently available. The large difference between this prediction and that of the same model using Cohen-Kurath wave functions demonstrates the sensitivity of spin observables to the choice of nuclear wave function used as input. In contrast, the cross sections seem independent of the wave function, as shown in parts (a) of the same figures.

Several possible reasons for the discrepancies among the models have been addressed in theoretical papers [9,10,12]. First, it is apparent from the poor description of the large-angle cross sections that the reaction mechanism is poorly understood at these angles. This is more than a lack of knowledge of the spin-flip amplitude since the problem exists at all large angles, not just near the minima of the cross section. Furthermore, it is more than a problem inherent in first-order optical model calculations, since it persists in the second-order calculations of Mach. Second, several approximations commonly used in the calculations may introduce inaccuracies. The most apparent of these is the treatment of Fermi motion of the nucleons [10]. None of the models discussed here treats Fermi motion in an exact way. Third, as mentioned above, there may be quenching of spin effects in π^- nucleus scattering. The magnitude of these effects can only be determined through more measurements. Fourth, Mach's work shows that predictions of spin observables exhibit strong dependence on the wave functions used as input. This can be seen in Fig. 4 where the same model produces very different results depending on the wave function used.

In addition, it is known that at energies near the Δ resonance, use of the free πN amplitudes alone is not sufficient to describe π-nucleus interactions [12]. This is precisely the reason for development of the Δ-hole model of nuclear interactions. (Even the values of the free πN amplitudes at energies below resonance are in doubt [24].) Unfortunately, no Δ-hole calculations of A_y are available for ^{13}C at $T_\pi = 100$ MeV.

We note in conclusion that the measurements reported here required an extraordinarily long running period and still the uncertainties in the resulting data are dominated by a lack of statistics. As a result, further measurements of A_y by this group will await completion of a 360° angular acceptance magnetic spectrometer being constructed at TRIUMF to facilitate measurements such as these.

ACKNOWLEDGMENTS

We thank S. Chakravarti, P. Siegel, and R. Mach for providing the results of their theoretical calculations. We gratefully acknowledge the help of the TRIUMF technical and support staff. This work was supported in part by the Natural Sciences and Engineering Research Council of Canada, and in part by the U.S. Department of Energy. One of the authors (E.F.G.) gratefully acknowledges partial support from a CSUS grant.

[1] R. Tacik *et al.*, Phys. Rev. Lett. **63**, 1784 (1989).
[2] R. Meier *et al.*, Phys. Rev. C **42**, 2222 (1990).
[3] S. Ritt *et al.*, Phys. Rev. C **43**, 745 (1991).
[4] Yi-Fen Yen *et al.*, Phys. Rev. Lett. **66**, 1959 (1991).
[5] J. Görgen *et al.*, Phys. Rev. Lett. **66**, 2193 (1991).
[6] D. J. Ernst and Kalvir S. Dhuga, Phys. Rev. C **37**, 2651 (1988).
[7] P. B. Siegel, private communication.
[8] D. J. Ernst, in *Proceedings of the LAMPF Workshop on Physics with Polarized Nuclear Targets,* edited by G. Burleson, W. Gibbs, G. Hoffmann, J. J. Jarmer, and N. Tanaka (Los Alamos National Laboratory Report No. LA-10772-C, 1986).
[9] S. Chakavarti, University of Minnesota Progress Report No. 19, 1990; and private communication.
[10] R. Mach and S. S. Kamalov, Nucl. Phys. **A511**, 601 (1990).
[11] L. S. Kisslinger and W. L. Wang, Ann. Phys. (N.Y.) **99**, 374 (1976).
[12] R. A. Freedman, G. A. Miller, and E. M. Henley, Nucl. Phys. **A389**, 457 (1982).
[13] TRIUMF Users Handbook (1987), p. IV-19.
[14] M. E. Sevior *et al.*, Phys. Rev. C **40**, 2780 (1989).
[15] G. R. Smith *et al.*, Phys. Rev. C **38**, 251 (1988).
[16] L. E. Antonuk *et al.*, Nucl. Phys. **A420**, 435 (1984).
[17] J. H. Mithcell, J. T. Brack, R. J. Peterson, R. A. Ristinen, J. L. Ullmann, R. L. Boudrie, B. G. Ritchie, and J. Escalante, Phys. Rev. C **37**, 710 (1988).
[18] S. J. Seestrom-Morris, D. Dehnhard, M. A. Franey, G. S. Kyle, C. L. Morris, R. L. Boudrie, J. Piffaretti, and H. A. Thiessen, Phys. Rev. C **26**, 594 (1982).

[19] T.-S. H. Lee and D. Kurath, Phys. Rev. C **21**, 293 (1980).
[20] W. B. Kaufmann and W. R. Gibbs, Phys. Rev. C **28**, 1286 (1983).
[21] S. Cohen and D. Kurath, Nucl. Phys. **A226**, 253 (1974).
[22] L. Tiator, Phys. Lett. **125B**, 367 (1983).
[23] I. S. Towner, Phys. Rep. **155**, 264 (1987).
[24] R. A. Arndt, Z. Li, D. Roper, and R. L. Workman, Phys. Rev. D **43**, 2131 (1991).